

Zig-zag magnetic ordering in honeycomb-layered $\text{Na}_3\text{Co}_2\text{SbO}_6$ Cheryl Wong^a, Maxim Avdeev^b, Chris D. Ling^{a,*}^a School of Chemistry, The University of Sydney, Sydney, NSW 2006, Australia^b Bragg Institute, B87, Australian Nuclear Science and Technology Organisation, Locked Bag 2001, Kirrawee DC, NSW 2232, Australia

ARTICLE INFO

Article history:

Received 3 May 2016

Received in revised form

9 July 2016

Accepted 31 July 2016

Available online 3 August 2016

Keywords:

Layered oxides

Honeycomb

Magnetic structure

Neutron diffraction

Zig-zag

ABSTRACT

$\text{Na}_3\text{Co}_2\text{SbO}_6$ is a layered oxide with a hexagonal O3-type structure, in which CdI_2 -type edge-sharing MO_6 octahedral layers are intercalated by Na. The MO_6 octahedral layer in turn adopts a honeycomb ordering pattern of magnetic ($S=3/2$) Co^{2+} sites surrounding isolated non-magnetic Sb^{5+} sites. Magnetic susceptibility measurements show that $\text{Na}_3\text{Co}_2\text{SbO}_6$ orders antiferromagnetically below $T_N=8.3$ K, with an effective magnetic moment of $5.22 \mu_B$ (indicating a strong orbital contribution above the expected spin-only value of $3.87 \mu_B$). While a honeycomb arrangement of magnetic cations could, in principle, support a co-operative long-range-ordered magnetic structure in which all nearest neighbors are antiferromagnetic with respect to one another, symmetry analysis of low-temperature neutron powder diffraction data shows that it instead adopts a partially frustrated 'zig-zag' ordering in which 2/3 of nearest-neighbor interactions are ferromagnetic and 1/3 are antiferromagnetic. The low Néel temperature and Weiss constant of $\theta = 2.2$ K underlines the presence of significant frustration of the expected strong superexchange interactions among Co^{2+} .

© 2016 Elsevier Inc. All rights reserved.

1. Introduction

Transition-metal oxides that are capable of intercalating small mobile ions such as Li^+ and Na^+ have been intensively studied for their electrochemical properties [1–3], but their magnetic properties remain relatively unexplored. Those with CdI_2 -type oxide layers such as LiCoO_2 [4,5], which are the most interesting for metal-ion battery cathode applications, have quasi two-dimensional triangular arrays of transition metals which are not conducive to long-range magnetic ordering. Nevertheless, in many cases they still show interesting properties, the most notable example being bulk superconductivity in $\text{Na}_x\text{CoO}_2 \cdot y\text{H}_2\text{O}$ [6,7].

When one-third of the transition metal cations are replaced with non-magnetic cations with significantly higher charges, such as Te^{6+} , Sb^{5+} or Bi^{5+} , an ordered hexagonal honeycomb lattice of magnetic cations results [8]. This is shown in Fig. 1 for the title compound $\text{Na}_3\text{Co}_2\text{SbO}_6$ [9,10], which adopts the O3 interlayer stacking sequence polytype [11] in which the Na cations occupy octahedral interstices.

The honeycomb topology supports long-range magnetic order of various types, including collinear nearest-neighbor antiferromagnetism (AFM). A significant number of such compounds have been synthesized, and although in the majority of cases only the lattice parameters have been reported, some have shown

evidence for long-range magnetic ordering. In addition to the title compound, these include $\text{Li}_3\text{Cu}_2\text{SbO}_6$ [12], $\text{Li}_3\text{Ni}_2\text{SbO}_6$ [13,14], $\text{Na}_3\text{Ni}_2\text{SbO}_6$ [15], $\text{Na}_3\text{Cu}_2\text{SbO}_6$ [16], $\text{Na}_2\text{Co}_2\text{TeO}_6$ [9,17], $\text{Na}_2\text{Ni}_2\text{TeO}_6$ [17,18], $\text{Na}_2\text{Cu}_2\text{TeO}_6$ [19], $\text{Li}_3\text{Ni}_2\text{BiO}_6$ [20] and $\text{Na}_3\text{Ni}_2\text{BiO}_6$ [21]. Another class of honeycomb systems that has attracted recent attention are the iridates, notably the 'harmonic' Li_2IrO_3 series [22–24], the corner-sharing Ir^{5+} compound $\text{Sr}_3\text{CaIr}_2\text{O}_9$ [25], and Na_2IrO_3 [26,27].

To date, the only magnetic structures that have been reported for honeycomb materials comparable to that investigated in the present work are those of $\text{Na}_3\text{Ni}_2\text{BiO}_6$ [21] (determined experimentally) and $\text{Na}_3\text{Ni}_2\text{SbO}_6$ [15] (determined theoretically), both of which are reported to adopt a 'zig-zag' magnetic ground state. This is one of three ordered AFM ground states proposed for the honeycomb lattice, which are summarized in Fig. 2. It has been proposed that the 'zig-zag' model is the most likely structure for the archetypal $J = 1/2$ honeycomb lattice Na_2IrO_3 [26], based on *ab initio* calculations. The stable state for a $J = 3/2$ system such as $\text{Na}_3\text{Co}_2\text{SbO}_6$ has not been tested in this way.

Here, we present the results of the first low-temperature neutron diffraction studies of long-range magnetic structure for $\text{Na}_3\text{Co}_2\text{SbO}_6$. The oxidation state of Co is expected to be $2+$ in both cases, noting that Sb is expected to be in its highest oxidation state of $5+$. $\text{Na}_3\text{Co}_2\text{SbO}_6$ should therefore be a good candidate for long-range order given the relatively strong magnetic interactions typically observed among high-spin Co^{2+} ($S = 3/2$) ions directly bridged by oxide ions.

* Corresponding author.

E-mail address: chris.ling@sydney.edu.au (C.D. Ling).

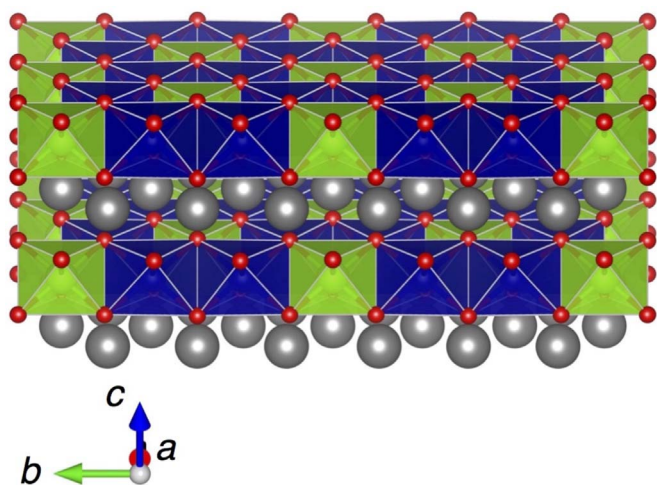


Fig. 1. Crystal structure of O3-type $\text{Na}_3\text{Co}_2\text{SbO}_6$ (monoclinic, $S.G. C2/m$). CoO_6 octahedra are blue, SbO_6 octahedra are green, O atoms are red and Na atoms are gray. The projection is chosen to highlight the 'honeycomb' distribution of Co around Sb in each layer. (For interpretation of the references to color in this figure legend, the reader is referred to the web version of this article.)

2. Experimental section

$\text{Na}_3\text{Co}_2\text{SbO}_6$ was synthesized using conventional solid state methods from stoichiometric mixtures of Na_2CO_3 (Merck, 99.9%), Co_3O_4 (Sigma-Aldrich, $<10\ \mu\text{m}$), and Sb_2O_3 (BDH Chemicals, 99%). The precursors were ground using an agate mortar and pestle, pressed into pellets, and sintered at $650\ ^\circ\text{C}$ in air for 12 h. Following intermittent regrinding and pressing, the sample was calcined in air at $900\ ^\circ\text{C}$ for 12 h.

The sample was confirmed to be single-phase using a PANalytical X'Pert PRO MPD X-ray powder diffractometer (XRD) in Bragg-Brentano geometry. The diffractometer was equipped with an unmonochromated $\text{Cu K}\alpha$ source ($\lambda_1 = 1.5406\ \text{\AA}$, $\lambda_2 = 1.5444\ \text{\AA}$) operating at 45 kV/40 mA. Data were collected over an angular range of $10^\circ < 2\theta < 80^\circ$ at a rate of $0.028^\circ\ \text{s}^{-1}$.

Synchrotron X-ray powder diffraction (SXRD) patterns were collected on the Powder Diffraction beamline (10-BM-1) at the Australian Synchrotron. The beam was calibrated using the NIST LaB_6 660b standard to a wavelength $\lambda = 0.825136(2)\ \text{\AA}$. Samples were loaded into 0.3 mm diameter glass capillaries and data collected using a MYTHEN microstrip detector over the 2θ range of $5^\circ < 2\theta < 80^\circ$, configured in Debye-Scherrer geometry. The crystal structure was refined using the Rietveld method as implemented in the GSAS program [28] with the EXPGUI front-end [29].

Temperature-dependent DC magnetic susceptibility, field-dependent magnetization and heat capacity measurements were made using a Quantum Design Physical Property Measurement System (PPMS). Susceptibility data were measured under zero

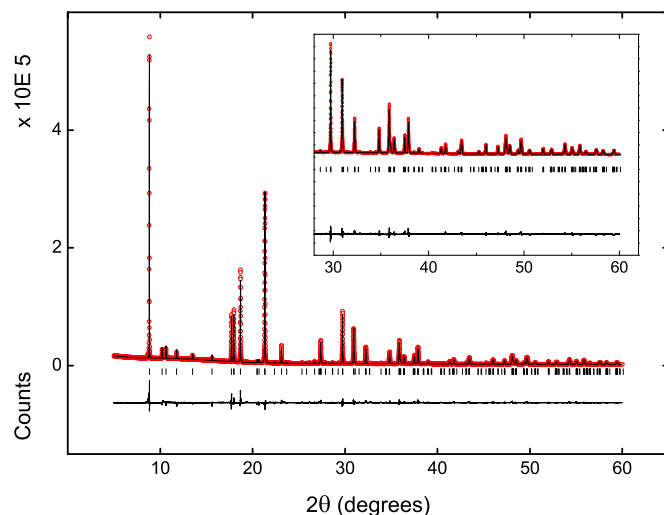


Fig. 3. Final Rietveld-refined fit to SXRD data ($\lambda = 0.825136(2)\ \text{\AA}$) for $\text{Na}_3\text{Co}_2\text{SbO}_6$. Observed (red dots), calculated (black line) and difference (blue line) patterns at low angles are shown. The inset highlights the high-angle data. (For interpretation of the references to color in this figure legend, the reader is referred to the web version of this article.)

field-cooled (ZFC) and field-cooled (FC) conditions in the temperature range of $2 < T < 300\ \text{K}$ using a coercive field of 0.1 T. Magnetization as a function of applied magnetic field was measured over the range of $-9 \leq H \leq 9\ \text{T}$ at constant temperatures of 2 and 40 K. Heat capacity measurements were collected over the temperature range of $2 < T < 50\ \text{K}$ under high vacuum.

Neutron powder diffraction (NPD) patterns were collected using neutrons of wavelength $\lambda = 2.4395\ \text{\AA}$ on the high-resolution powder diffractometer Echidna at the OPAL facility operated by ANSTO. A $\sim 5\ \text{g}$ powdered sample was loaded into a 9 mm diameter cylindrical vanadium can. Data were collected between 1.5 and 40 K using an 'orange' cryostat. The magnetic structure was analyzed using the Fullprof Suite [30] with the default neutron scattering lengths and the Co^{2+} magnetic form factor.

3. Results and discussion

The peaks in SXRD patterns of $\text{Na}_3\text{Co}_2\text{SbO}_6$ were all accounted for by a single phase, confirming the purity of the sample. The final Rietveld fits to these data are presented in Fig. 3. The refined unit cell is within the ranges of reported values in the literature, given in Table 1. The reported values vary significantly, which can be attributed to slight variations in the Na stoichiometry: reduced Na content weakens inter-layer interactions and expands the c -axis; while consequent partial oxidation of Co decreases the average cation size (and *vice versa*). The fact that our sample has both a smaller unit cell and a higher magnetic ordering temperature

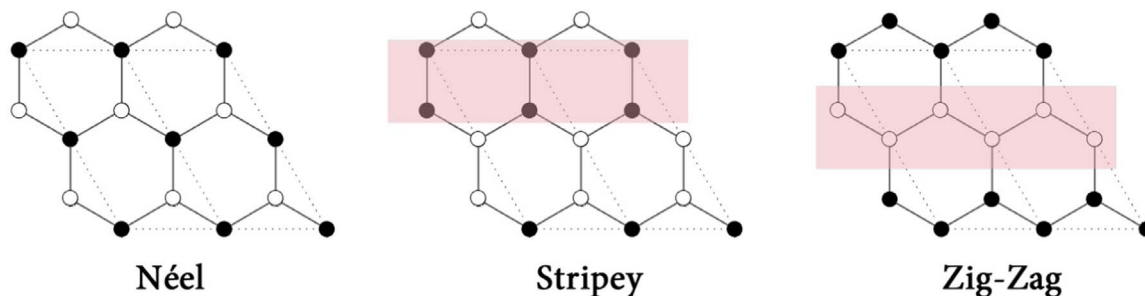


Fig. 2. Schematic illustrating possible AFM ordering patterns for magnetic cations on a honeycomb lattice (adapted from Liu et al. [26]). The black and white atoms indicate up and down spin, respectively. Dashed lines show the hexagonal unit cell of Na_2IrO_3 .

Download English Version:

<https://daneshyari.com/en/article/1329392>

Download Persian Version:

<https://daneshyari.com/article/1329392>

[Daneshyari.com](https://daneshyari.com)